Numerical Calculation of Wall Erosion on Hall Thrusters Using 2D-Hybrid-PIC Modeling

IEPC-2007-200

Presented at the 30th International Electric Propulsion Conference, Florence, Italy
September 17-20, 2007

Hiroyuki Koizumi*
Institute of Space and Astronautical Science / Japan Aerospace Exploration Agency
Yoshinodai, Sagamihara, Kanagawa 229-8510, JAPAN

and

Kimiya Komurasaki†, and Yoshihiro Arakawa‡
University of Tokyo, Hongo, Bunkyo-ku, Tokyo 113-8656, Japan

Hall thrusters are promising space propulsion options for spacecraft. Current major interest in Hall thrusters is their life time evaluation for long time operation. Sputtering erosion of the insulation wall determines the life time of the thrusters. In this study, we present two-dimensional Hybrid-PIC modeling of Hall thrusters, which predicts the wall erosion effect. The principle challenges of our modeling is 1) solving both the plasma generation and acceleration in the channel and the exhaust plume in the near field of the exit and 2) predicting the channel erosion by ion sputtering with deforming the calculation grid.

Nomenclature

e	=	elementary electric charge
k	=	Boltzmann constant
m	=	particle's mass
n	=	number density
$\hat{n}$	=	coordinate perpendicular to the magnetic field
S	=	heat source terms in the electron energy equation
T	=	electron temperature
t	=	time
v	=	velocity
ε	=	electron energy
λ	=	stream function of the magnetic field
μ	=	electron mobility
φ	=	electric potential
φ^*	=	thermalized electric potential
e, i, n	=	electron, ion, and neutral particle
$\perp$	=	perpendicular to the magnetic field

* Research Associate, Department of Space Transportation Engineering, koizumi.hiroyuki@jaxa.jp
† Associate Professor, Department of Advanced Energy, komurasaki@k.u-tokyo.ac.jp
‡ Professor, Department of Aeronautics and Astronautics, arakawa@al.t.u-tokyo.ac.jp

I. Introduction

Hall thrusters are space propulsion devices which accelerate ionized propellant gas by electrostatic force. They have high thrust efficiency of over 50 % with the specific impulse of 1000 – 2000 s and high thrust density enabling compact propulsion system. Because of these advantages, Hall thrusters are suitable to the application to station keeping and attitude control of near-Earth satellite. Because these satellites are useful for the commercial use, the development of Hall thrusters for that field is promising..

To date, Hall thrusters have been studied in detail experimentally, and robust design guide have been established by empirical method. For instance, magnetic field profiles and channel geometries appropriate for the thrusters are roughly known in the researchers. However, design support methods which can predict the thruster performance, their spacecraft contamination, and life time of the thruster have not been established yet. Hall thrusters conduct plasma generation and the acceleration in the same channel, and it makes analytical prediction of the performance difficult. Additionally it is also difficult to experimentally investigate the contamination and life time problem by the ground test. To solve these problems numerical modeling of Hall thrusters is necessary.

Recently, several numerical models of Hall thrusters have been developed. There are many numerical methods to simulate the thruster and the researchers have selected a method suitable to their objectives. Generally these numerical models can be categorized by the dimension of the calculation and the treatment of the particles. Three dimensional system would be ideal to simulate the physics in the thrusters, but it usually takes too much calculation cost. Two dimensional system, *r-z* or *r-θ* system, is frequently employed to reduce the cost. The former, assuming axial symmetry, calculates ion acceleration and electron stream along the axial direction to simulate the performances of the thrusters. The latter system is sometimes used to understand anomalous electron mobility, by calculating the azimuthal electrostatic wave which induces the electron drift along the axial direction. In the acceleration channel and near field plume, heavy particles (ions and neutral particles) hardly collide with each other. Hence they are usually described using particle simulations. On the other hand, electrons are strongly affected by the magnetic field and can be assumed that they are thermalized along the field lines. As a result the cross field electron transfer can be described by fluid equations. This assumption would not be correct in all the case, but it can significantly reduce the calculation cost. Then this is frequently assumed to describe the electron behavior in the thrusters. After all, to fully understand the physics in the thruster, three dimensional fully particle or kinetic simulation would be the best. However, this method takes enormous calculation cost even if using recent parallel computing, and it is not appropriate to support the design of the thrusters. In the view point of both the practical use and calculation cost for design guide system, 2D-Hybrid model would be the most appropriate. Details of the 2D-Hybrid model are shown in the reference [1-4].

In this study, we have developed a transient 2D-Hybrid numerical modeling to be utilized for the design support tools of Hall thrusters. The objectives of this numerical code are the prediction of the thruster performance, contamination to the spacecraft, and life time by the wall erosion. Particularly, this study focuses on the life time evaluation, and the numerical model was developed to describe the wall erosion by ion sputtering. The principal challenges of our modeling are 1) solving both the plasma generation and acceleration in the channel and the exhaust plume in the near field of the exit and 2) predicting the channel erosion by ion sputtering with deforming the calculation grid. Additionally, this numerical code predicts current-voltage characteristics, generated thrust and its divergence, and current oscillation characteristics as well as the other numerical modeling.

II. Numerical Modeling

A. Calculation Domain

The numerical calculation in this study models a Hall thruster developed in University of Tokyo. Figure 1 shows the picture of the thruster and calculation domain of this calculation. The acceleration channel has the outer and inner diameters of 31 and 24 mm and the length 25 mm, where 21 mm from the exit is covered with the insulation wall and the bottom 4 mm part is covered with anode. The insulation walls of the acceleration channel are made of boron nitride (BN) with the temperature of 800 K. Outside the channel, cylindrical space with the outer diameter of 60 mm and axial length of 35 mm away from the exit was calculated as the near field region.. The details of the configuration and operating characteristics are referred elsewhere [5].

B. Heavy particles

Motion of the ions and neutral particles are solved by a particle in cell method (PIC). Neutrals move in uniform linear motion and ions are accelerated by the electric field. The accelerating motion of the ions was solved using

predictor-corrector method. Densities of the neutral particles and ions are calculated at the node point of the cells. Neutrals are introduced from the bottom wall of the acceleration channel with the Maxwellian distribution. We consider xenon as the working gas and assumed the temperature as 800 K, which is considered to be equal to the wall temperature. Ions are generated based on the electron-neutral ionization collision, assuming electrons' Maxwellian distribution. To reduce the computational noise due to PIC, variable mass method was employed. Hence at least one macro-particle of the ion is generated in all the cell at every time step. Collisions between ions and neutrals were neglected because their mean free passes are much longer than the characteristic length of the thruster channel.

C. Electrons

Electrons are considered that they are thermalized along the magnetic field line with Maxwellian distribution. Therefore thermalized potential: ϕ^* and electron energy: ε are constant along the line. These two constants are obtained every time step by solving the conservation relations of the electron transportation across the field lines. Electric potential and field was calculated by the relation

$$\phi(r,z) = \phi^*(\lambda) + \frac{2\varepsilon(\lambda)}{3e}\ln\left(\frac{n(r,z)}{n_0}\right) \tag{1}$$

using the plasma density (ion density): n(r,z) calculated by PIC.

Cross field electron mobility is an important parameter which largely affect the profile of the thermalized potential and electron energy. It is known in the researchers of Hall thrusters that the classical description of the mobility predicts the current far below that obtained by experiments. A number of models to explain the enhanced mobility have been developed. The primary causes are considered as Bohm diffusion and electron wall collision. Particularly the former has larger effect than the latter in the most cases. The Bohm diffusion is based on the electron drift by the azimuthal electrostatic wave which can exist only in the region where the magnetic field is decreasing. Hence the Bohm diffusion was applied to the region further downstream than the peak point of the magnetic field. Wall collision effect was employed based on the Kozlov's theory [6].

D. Electric Field and Electron Energy

Plasma approximation was employed because we did not consider high frequency phenomena as plasma oscillation. Hence electric field was determined using not Poisson's equation but current conservation. Figure 2 shows the magnetic field used in this calculation, which was calculated using a commercially available magnetic

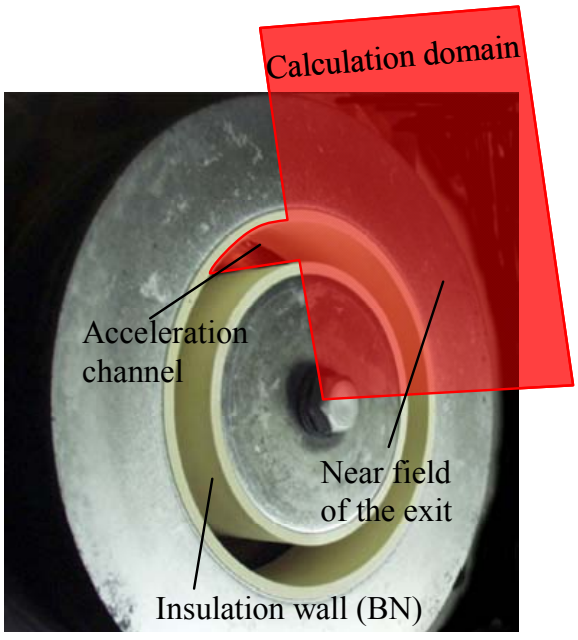

Fig.1 UT Hall thruster and the calculation domain.

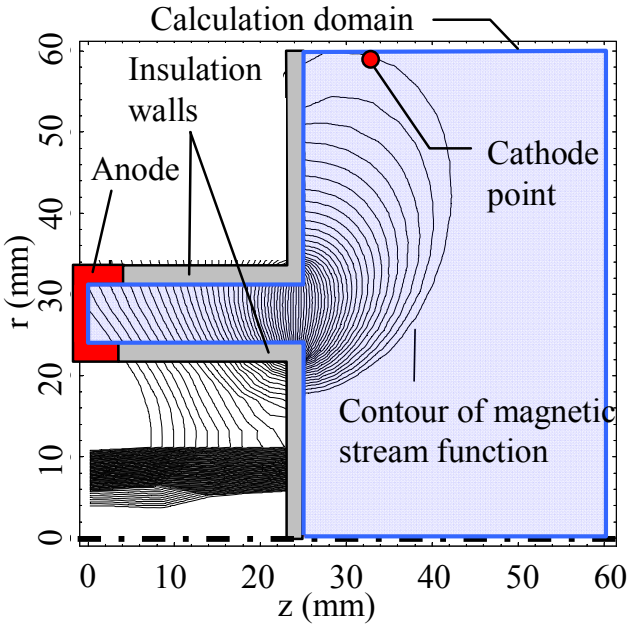

Fig. 2 Configuration of the magnetic field of UT Hall thruster (contour lines of the flux function).

field solver. Current conservation: $\nabla \cdot (-nv_i + nv_e) = 0$ was integrated in every flux tube, and simultaneous equation of the thermalized potential is obtained. The equation was solved using the Gaussian elimination method.

The electron energy along the line was obtained by solving the transport equation of the energy:

$$\frac{\partial}{\partial t}\int_{V_i} n\varepsilon dV + \int_{S_{i+1/2}} - \int_{S_{i-1/2}} \left(\frac{5}{3} n v_{e\perp}\varepsilon - \frac{5}{9e} n\mu_{e\perp}\varepsilon \frac{\partial \varepsilon}{\partial \hat{n}}\right) dS = \int_{V_i} (S_{Joule} - S_{wall} - S_{inel}) dV \quad (2)$$

This equation becomes simultaneous equation of the electron energy and it was solved as well as the energy conservation.

E. Wall Erosion

PIC calculation of this study was coded to be adapted to an arbitrary-shaped walls in the acceleration channel. Figure 3 shows the conceptual diagram of gridding patterns between walls curved in a arbitrary shape. The grid system was equally divided between the outer and inner walls, which makes trapezoid cells as shown in the Fig.3. By employing this gridding method, this numerical code can calculate Hall thrusters with arbitrary shaped wall. For example, Fig. 4 is the calculation result of the thruster with the sinusoidal channel wall. This geometry does not any practical meaning but it is developed just for the demonstration of this coding. Even using this kind of a curious wall shape, the calculation successfully worked.

One of the serious problems about the prediction of the sputtering erosion is poor data on the low energy sputtering. Generally, Hall thrusters accelerate the ions up to 200 – 300 eV. Hence in the acceleration channel, ions collide to the wall below that energy, and sputter yield in such low energy is required to predict the wall erosion rate. However, there is a few research which investigated the sputter yield of xenon vs BN in such low energy level. In this study, we have used the data reported by Gainer et al. and Kim et al.[7-8]. Figure 5 shows the energy dependence and angular dependence of the sputter yield dealt here. Sputter yield is the function of the both energy and incident angle: $Sy(E,\theta)$. Also it is known that normalized sputter yield $Sy^*(\theta) = Sy(E,\theta)/ Sy(E,0)$ is almost independent on the energy. In that case, the sputter yield can be written as $Sy(E,\theta) = Sy^*(\theta)\ Sy(E,0)$. Here we used this relation using the fitted curve in Fig. 4.

After all calculation of the wall erosion was carried out as follows. First, transient 2D-Hybrid calculation was solved, where the time step for the PIC calculation was 0.1 μs. After the convergence to a steady state, energy and angular distribution of the ions impacted to the wall was obtained, where the distribution was

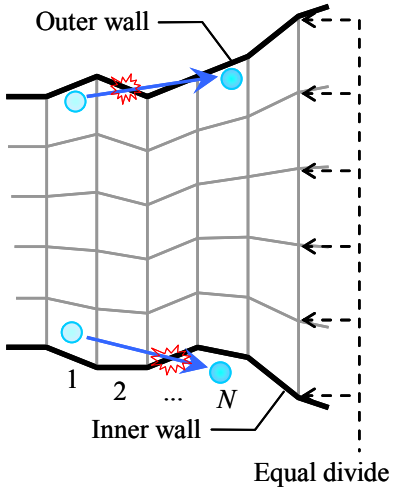

Fig.3 Conceptual diagram of the gridding pattern in the arbitrary-shaped walls.

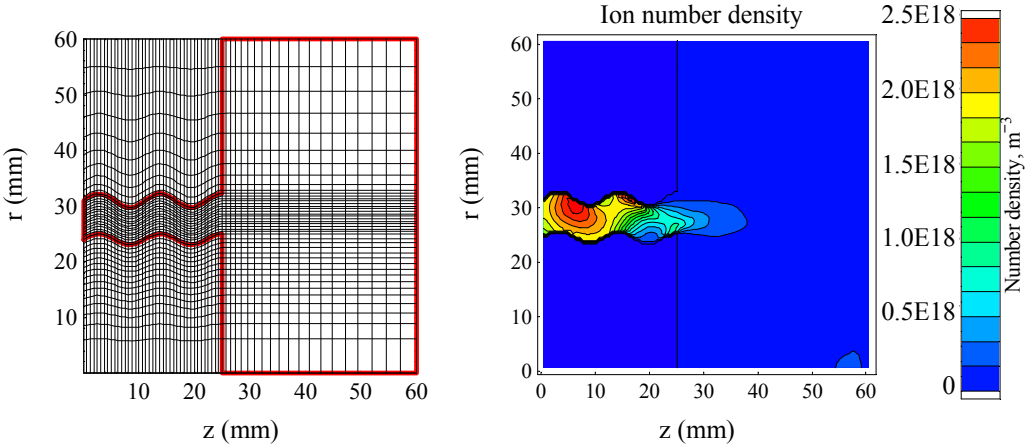

Fig.4 Calculation results of 2D-PIC Hybrid code with a sinusoidal-shaped channel wall, demonstration calculation of the code.

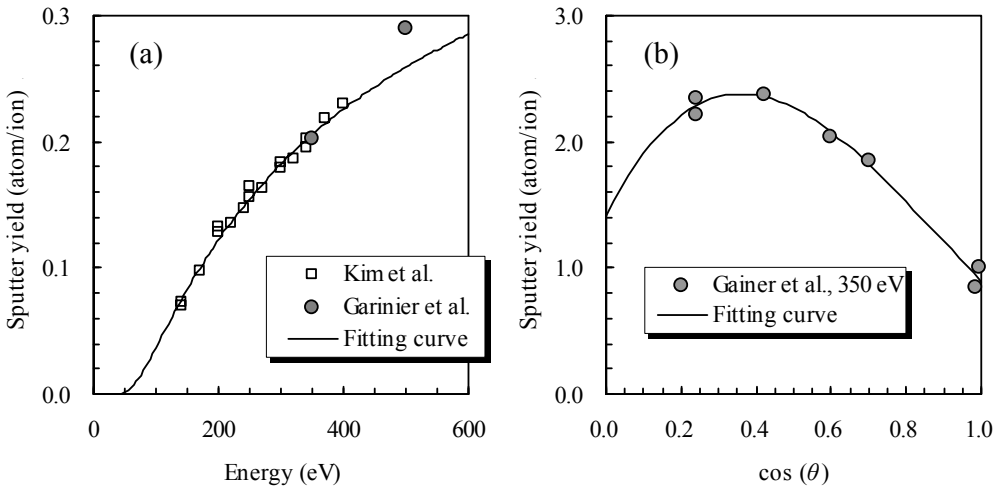

Fig.5 Sputter yield of Xe vs BN used here; (a) Energy dependence at normal incident and (b) Angular dependence of normalized sputter yield.

averaged over 450 μs to reduce the computational noise. The wall erosion rate was calculated using the above ion distributions and tabulated data of the BN sputter yield. Based on the erosion rate, new wall shapes of certain hours later was determined. To improve the accuracy of the time integration, Adams-Bashforth scheme using non-constant time step was used. Namely, wall erosion increment: $\Delta R_{i+1/2}$ from i to i+1 erosion time step was obtained as

$$\Delta R_{i+1/2} = \frac{\Delta T_i(\Delta T_i + \Delta T_{i-1})}{2\Delta T_{i-1}}\left\langle \frac{dr}{dt} \right\rangle_i - \frac{\Delta T_i^2}{2\Delta T_{i-1}}\left\langle \frac{dr}{dt} \right\rangle_{i-1} \tag{3}$$

$$\left\langle \frac{dr}{dt} \right\rangle_i = \frac{M_{BN}}{2\pi r \rho_{BN} N_A}\left\langle \iint f(E,\theta) Sy(E,\theta) dE d\theta \right\rangle_i \tag{4}$$

where ΔT_i is erosion time step from i to i+1, $< >_i$ means the time average in the time step i, M_{BN} and ρ_{BN} are molecular weight and density of BN, $f(E,\theta)$ is ion distribution function on the energy and the angle which collide with the wall. The time step ΔT_i was successively determined such that the maximum erosion rate does not exceed 100 μm. As a result, ΔT was changed from about 10 h in the first stage of the calculation (< 300 h) to about 40 h in the later stage (> 1000 h). Calculation was carried out again using these new walls. Above sequences are repeated to obtain the eroded wall shape. 2D-Hybrid code using arbitrary-shaped wall and sputter yield data of the wall material (BN) are necessary to conduct the above calculation.

III. Results

In this section, we show the calculation results under the typical condition of voltage 250 V, mass flow rate of 1.0 Aeq (xenon), and maximum field strength of 12.7 mT in the channel. In this condition, the discharge current was stable (not oscillated), but in the higher field discharge oscillation started. Figure 6 shows typical current histories calculated in the magnetic field of 12.7 mT and 19.1 mT. It is shown that discharge current is strongly oscillating in the higher

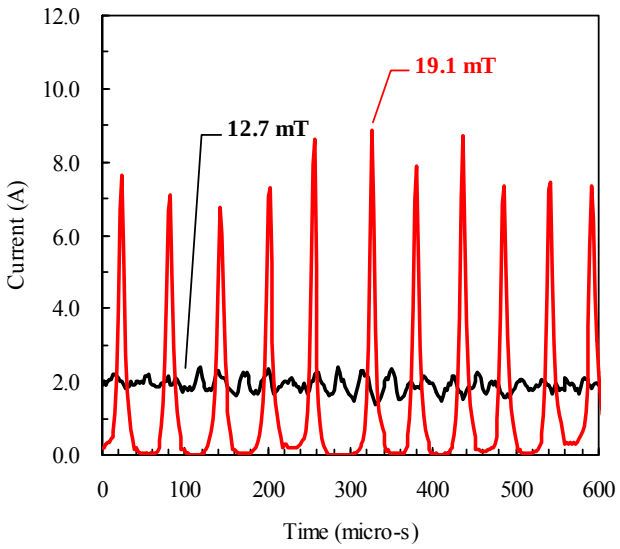

Fig.6 Time histories of the discharge current, calculated with the maximum magnetic field strength of 12.7 and 19.1 mT.

magnetic field. Hall thrusters are usually operated by selecting the condition with high performance (low current, high magnetic field) but with no oscillation. Therefore we selected the above condition (12.7 mT) as the standard condition for the erosion calculation, although this time-depending numerical model can be used to assess the problem of the current oscillation.

Figure 7 – 10 shows evolution of the gridding pattern and profiles of several quantities (electric potential, neutral density, and ion density) by the erosion calculation. In the figures, grids and profiles after 0 h (1st erosion time step), 508 h (45 steps), 1002 h (68 steps), and 2021 h (96 steps) are shown. The results after 0 h are the calculation using a usual straight channel wall. The electric potential lines deviates from the magnetic field lines because of the second term of the thermalized potential. The potential lines are almost perpendicular to the channel walls whereas the field lines has slight inclination to them towards the outward in the farther upstream region than the peak point of the magnetic strength. This corresponds to the profile of the plasma density whose maximum point located in a little outward of the center of the channel. Ions have the maximum density in the middle of the acceleration channel and just upstream of the potential drop. In the further downstream, the density is dropping by the acceleration in the axial direction. In the near-field plume, there is a bunch of the ions near the center axis. These ions are generated in the near-field but not accelerated by the electric potential. Although generation (ionization) of these ions is very low, they have much time to stay there due to their low velocity.

Wall erosion by ion sputtering and the successive calculation using the deformed walls was successfully solved. Deformation of the walls affected the profile of the plasma potential and density. The sputtering erosion occurred in the region from the channel exit to 10 mm upstream. This region is corresponding to the potential drop. Low energy ions which have the temperature equal to the wall cannot cause the wall sputtering, because there is an energy threshold of the sputter yield. Therefore in the upstream of the channel there was not sputtering erosion, whereas there are a lot of ions. Particularly the wall erosion was significant on the outer wall, which expanded up to 37.9 mm from 31.0 mm at the exit. On the other hand the inner wall was from 24.0 mm to 22.2 mm. This difference would be caused by the magnetic field configuration and resulted ion profile in the channel. In this work, this erosion can not be quantitatively evaluated, because there was no experiment data of the channel erosion about the thruster modeled here. In the case of a different thruster, for instance, SPT-100 thruster showed the wall erosion of 5 mm and 8 mm on the both walls after 2000 h operation [9]. Considering the difference of the power and dimensions, the erosion of this simulation would be appropriate. In the next step of this work, quantitative validation of our result should be conducted by modeling the known thruster like SPT-100 or performing the endurance test of other thrusters.

IV. Conclusion

Numerical modeling of a Hall thruster was conducted using 2D-Hybrid-PIC method to calculate sputtering wall erosion of the acceleration channel and predict the successive change of the electrical potential, neutral density, and ion density profiles. As a result of long time (2000 h) simulation, it was shown that it can calculate wall erosion and successive operation under the sputtered channel walls.

Acknowledgments

The present work was supported by a Grant-in-Aid for Scientific Research (S), No. 16106012, sponsored by the Ministry of Education, Culture, Sports, Science and Technology, Japan.

References

[1] J.M. Fife; Ph.D. thesis, Massachusetts Institute of Technology, 1998.
[2] M.K. Allis, N.G. Gascon, C.V. Goudou, and M.A. Cappelli, and E. Fernandez; *40th Joint Propulsion Conference*, Ft. Lauderdale, FL, July 11-14, 2004, AIAA-2004-3951.
[3] G.J. Hagelaar, J. Bareilles, L. Garrigues, and J.P. Boeuf; *J. App. Phys.*, Vol.91-9, 2002, p5592-5598.
[4] J.W. Koo and I.D. Boyd; *Compu. Phys. Commun.*, Vol.164, 2004, p442-447.
[5] N. Yamamoto, K. Komurasaki, Y. Arakawa; *J. Propulsion and Power*, Vol.21-5, 2005, p870-876.
[6] A.N. Kozlov; *Plasma Phys. Rep.*, Vol.28-2, 2002, p180-187.
[7] Y. Garnier, V. Viel, J.F. Roussel, and J. Bernard; *J. Vac. Sci. Technol. A*, Vol.17-6, 1999, p3246-3254.
[8] V. Kim, V. Kozlov, A. Semenov, and I. Shkarban; *27th International Electric Propulsion Conference,* Pasadena, CA, October 15-19, 2001, IEPC-01-073.
[9] C.E. Carner, J.R. Brophy, J.E. Polk, and L.C. Pless; *30th Joint Propulsion Conference*, Indianapolis, IN, June 27-29, 1994, AIAA-1994-2856.

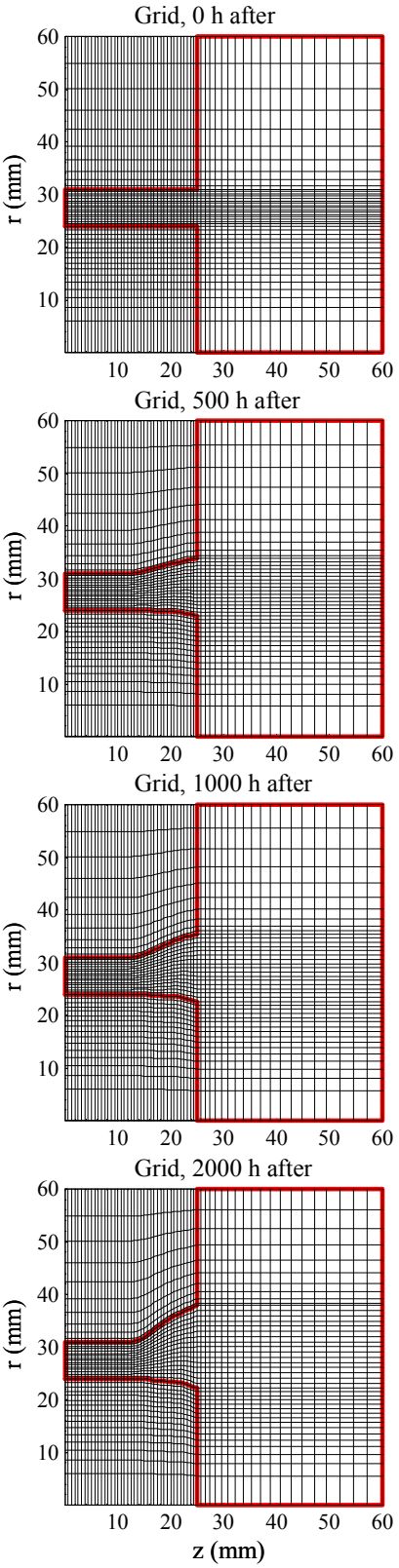

Fig.7 Deformation of the gridding pattern by the sputtering erosion; 0, 500, 1000, and 2000 h after the initial operation.

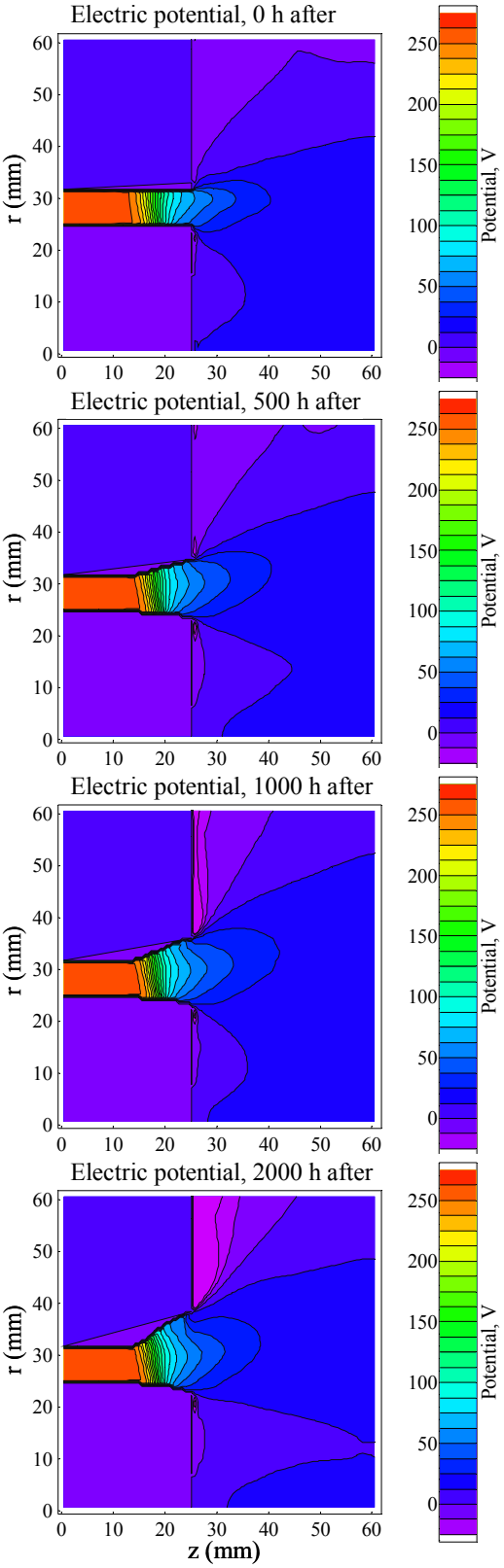

Fig.8 Evolution of the electric potential by the wall deformation; 0, 500, 1000, and 2000 h after.

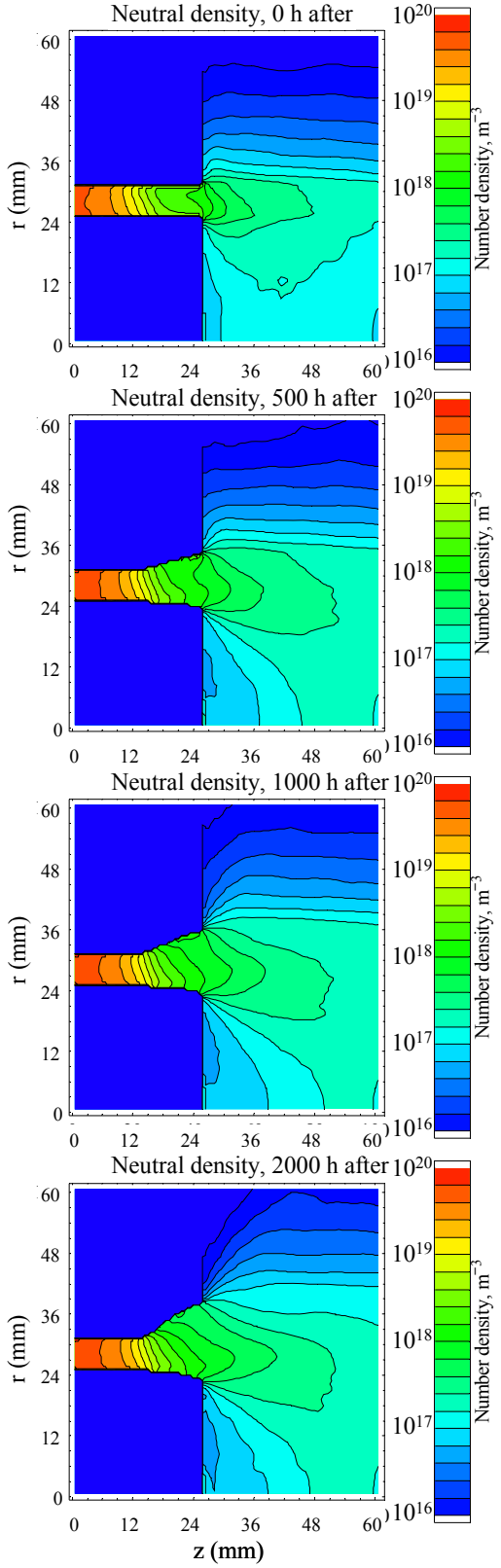

Fig.9 Evolution of the neutral density profile (contour plot of the log scale) by the wall deformation; 0, 500, 1000, and 2000 h after.

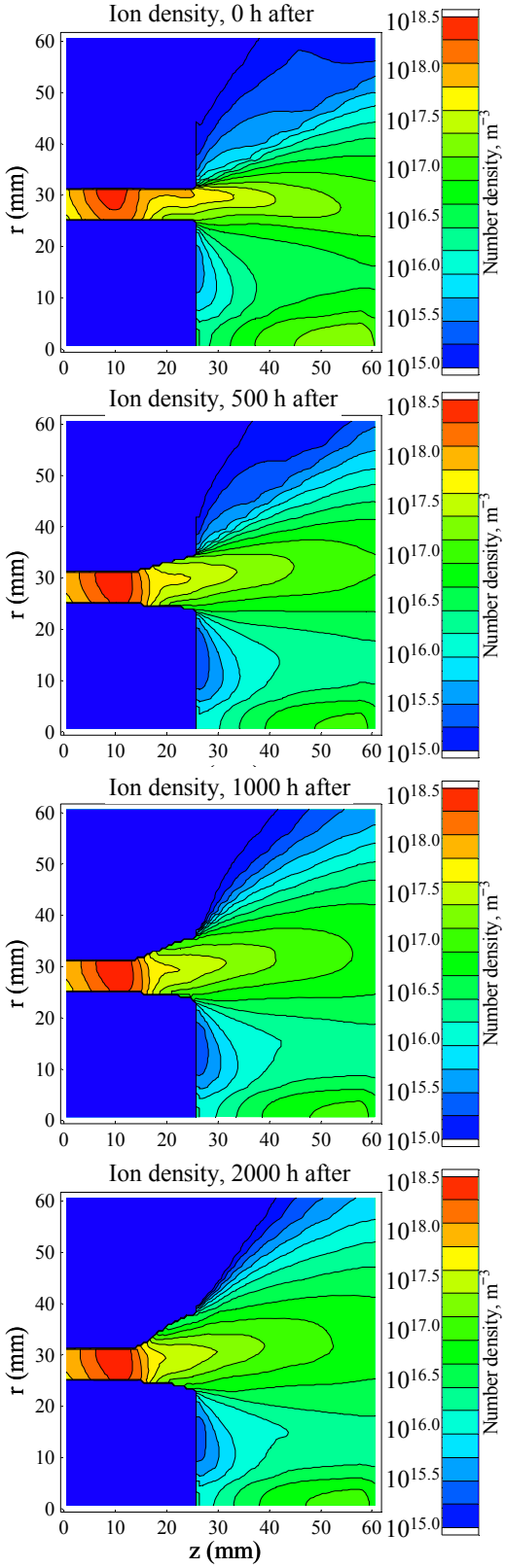

Fig.10 Evolution of the ion density profile (contour plot of the log scale) by the wall deformation; 0, 500, 1000, and 2000 h after.